

Efficient CRISPR/Cas9 genome editing with low off-target effects in zebrafish

Alexander Hruscha¹, Peter Krawitz^{2,3,4}, Alexandra Rechenberg¹, Verena Heinrich², Jochen Hecht^{3,4}, Christian Haass^{1,5,6} and Bettina Schmid^{1,6,*}

ABSTRACT

Gene modifications in animal models have been greatly facilitated through the application of targeted genome editing tools. The prokaryotic CRISPR/Cas9 type II genome editing system has recently been applied in cell lines and vertebrates. However, we still have very limited information about the efficiency of mutagenesis, germline transmission rates and off-target effects in genomes of model organisms. We now demonstrate that CRISPR/Cas9 mutagenesis in zebrafish is highly efficient, reaching up to 86.0%, and is heritable. The efficiency of the CRISPR/Cas9 system further facilitated the targeted knock-in of a protein tag provided by a donor oligonucleotide with knock-in efficiencies of 3.5–15.6%. Mutation rates at potential off-target sites are only 1.1–2.5%, demonstrating the specificity of the CRISPR/Cas9 system. The ease and efficiency of the CRISPR/Cas9 system with limited off-target effects make it a powerful genome engineering tool for *in vivo* studies.

KEY WORDS: C9orf72, CRISPR/Cas9, Genome editing, Knock in, Off-target, Zebrafish, Tardbp

INTRODUCTION

The induction of targeted mutations in zebrafish and other model organisms has only become possible through the use of genome editing tools, which induce mutations through DNA double-strand breaks and error-prone repair by non-homologous end joining. So far, genome editing has mostly been performed with zinc-finger nucleases (ZFNs) or transcription activator-like effector nucleases (TALENs). ZFNs can work very efficiently in zebrafish, but are expensive, difficult to design and function in a context-dependent manner, making initial *in vitro* testing mandatory (Carroll, 2011). TALENs are easy to design but require laborious cloning steps (Joung and Sander, 2013). The prokaryotic clustered, regularly interspaced, short palindromic repeats (CRISPR) and the CRISPR-associated system (Cas) (CRISPR/Cas system) is a very attractive alternative since it is the only genome engineering tool described so far that relies on Watson-Crick base pairing rather than the potentially less specific protein-DNA interaction (Gaj et al., 2013). The CRISPR/Cas system is derived from bacteria and archaea, where it is used as an innate immune strategy to inactivate foreign

intruding nucleic acids (Wiedenheft et al., 2012). The CRISPR locus consists of short palindromic repeats and short interspersed sequences of foreign DNA. Upon transcription, they serve as guide RNA (gRNA) to identify foreign DNA and target it for inactivation by nuclease-mediated cleavage. The CRISPR/Cas9 type II system of *Streptococcus pyogenes* has been optimized and successfully used in vertebrate cells to edit genomes (Cho et al., 2013; Horvath and Barrangou, 2013; Jinek et al., 2013; Mali et al., 2013; Shen et al., 2013; Wang et al., 2013). Recently, it has been further demonstrated to efficiently generate insertions and deletions due to incorrect repair by non-homologous end joining of induced double-strand breaks in zebrafish (Chang et al., 2013; Hwang et al., 2013a; Hwang et al., 2013b; Jao et al., 2013). We now demonstrate that the CRISPR/Cas9 system is highly efficient and specific in generating heritable mutations and knock-in (KI) alleles in zebrafish with negligible off-target effects.

RESULTS AND DISCUSSION

We designed four single-stranded gRNAs composed of the targeting sequence followed by the CRISPR sequence (supplementary material Fig. S1A) that guides the Cas9 nuclease to the desired genomic locus (Fig. 1A) (Jinek et al., 2012). gRNAs were designed to target the *tardbp* (*bpt1*), *tardbpl* (*bplt4*) and *C13H9orf72* (*C9t2* and *C9t3*, targeting distinct sites) genes (Fig. 1B; supplementary material Fig. S1A,B). The gRNAs were obtained by *in vitro* transcription directly from synthesized oligonucleotides (*C13H9orf72*), PCR products (*tardbp*) or plasmids (*tardbp*, *tardbpl*, *C13H9orf72*) as templates yielding comparable RNA quality. Since gRNA can be directly transcribed *in vitro* from synthetic oligonucleotides with similar efficiencies, laborious cloning procedures can be omitted (Fig. 1A). To demonstrate the efficiency of the CRISPR/Cas9 system in zebrafish we chose the *tardbp* and *tardbpl* genomic loci, which we identified as suitable and accessible for ZFN in a previous study (Schmid et al., 2013). The gRNA was co-injected with Cas9 mRNA from *Streptococcus pyogenes* (Jinek et al., 2012), to which we added two nuclear localization signals (NLSs) to target it to the nucleus (supplementary material Fig. S1C) (Cong et al., 2013), into fertilized one-cell stage embryos. Injected embryos were analyzed 24 hours post-fertilization (hpf) for genome modifications of the target locus. PCR products including the target site were amplified and analyzed by restriction fragment length polymorphism (RFLP) for induction of mutations (Schmid et al., 2013; van Bebber et al., 2013) (Fig. 1B). Sequence analysis confirmed that the loss of the respective restriction site was due to mutations at the target sites in the gRNA/Cas9-injected embryos.

We next tested gRNAs for two novel target sequences within *C13H9orf72* (*C9t2*, *C9t3*) (supplementary material Fig. S1B). A hexanucleotide repeat expansion in the first intron of the *C9orf72*, the human ortholog of *C13H9orf72*, has recently been shown to be causative for most cases of familial frontotemporal lobar

¹German Center for Neurodegenerative Diseases (DZNE), Schillerstrasse 44, 80336 Munich, Germany. ²Institute for Medical Genetics and Human Genetics, Charité Universitätsmedizin, 13353 Berlin, Germany. ³Berlin Brandenburg Center for Regenerative Therapies, Charité Universitätsmedizin, 13353 Berlin, Germany. ⁴Max Planck Institute for Molecular Genetics, 14195 Berlin, Germany. ⁵Adolf-Butenandt-Institute, Biochemistry, Ludwig-Maximilians University Munich, Schillerstrasse 44, 80336 Munich, Germany. ⁶Munich Cluster for Systems Neurology (SyNergy), 80336 Munich, Germany.

*Author for correspondence (bettina.schmid@dzne.de)

Received 17 May 2013; Accepted 25 September 2013

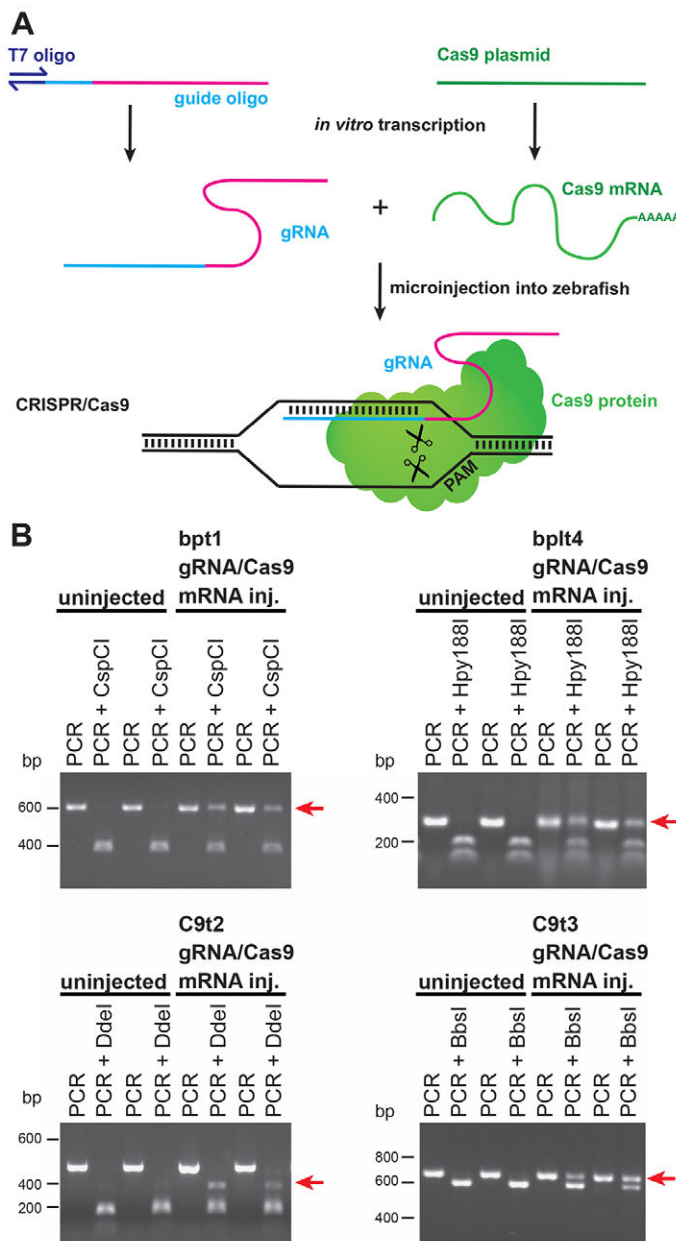


Fig. 1. Overview of the CRISPR/Cas9 system and mutation analysis of injected P0 founder embryos. (A) Guide oligonucleotides containing a T7 RNA polymerase binding site were annealed with T7 primer (blue). gRNA with a target binding site (cyan) was *in vitro* transcribed with T7 RNA polymerase. gRNA and Cas9 mRNA were co-injected into zebrafish embryos. The gRNA detects the endogenous genomic target site and can base pair via its target binding site, recruiting Cas9 protein (green) to induce a double-strand break at the target site (indicated by scissors) close to the protospacer adjacent motif (PAM). (B) PCR and restriction enzyme analysis of individual P0 embryos injected with bpt1, bpt4, C9t2 or C9t3 gRNA and Cas9 as indicated. PCR products are shown undigested (PCR) or after digestion with the appropriate restriction enzyme as indicated. Lanes 1-4 show uninjected siblings, whereas lanes 5-8 represent individual P0 founder embryos injected with the indicated gRNA/Cas9 mRNA. Red arrows indicate loss of restriction sites due to genomic mutations.

degeneration and amyotrophic lateral sclerosis (DeJesus-Hernandez et al., 2011; Renton et al., 2011; Gijssels et al., 2012). The repeat-expanded allele is transcribed at substantially reduced levels, suggesting that haploinsufficiency contributes to disease

pathogenesis (Gijssels et al., 2012; Mori et al., 2013). However, knockout (KO) animal models are not yet available to test this hypothesis. C9t2 and C9t3 gRNA/Cas9-injected P0 embryos were efficiently mutagenized (Fig. 1B; supplementary material Fig. S1D). For further phenotypic characterization it is essential to generate identical mutations in every cell of the animal. This can only be achieved after germline transmission of mutations of the injected founder fish, which is genetically mosaic (supplementary material Fig. S2). To determine germline transmission rates of CRISPR/Cas9, we raised C9t3 gRNA/Cas9 mRNA-injected and C9t2 gRNA/Cas9 mRNA-injected embryos to adulthood (P0) and screened their offspring (F1) for germline transmission (Fig. 2A-C). Of the seven C9t3 F1 clutches analyzed, we identified three clutches (43%) with a potential mutation in one allele of the target sequence by RFLP (Fig. 2A,B). For the C9t2 locus we screened 20 F1 clutches and identified four that carried a mutation (20%) (Fig. 2C). This germline transmission efficiency is comparable to the 45% average germline transmission that we previously observed with 12 different ZFNs (CompoZr, Sigma) (Schmid et al., 2013; van Bebber et al., 2013) (our unpublished observations). Of the seven positive F1 clutches, on average 11% (4-20%) of the 24 tested embryos carry a mutant allele. Sequencing of the non-digested PCR products consistently revealed indel mutations at the target site (Fig. 2B,C). C9t3 founder 4 propagated a 5 bp and a 445 bp deletion through the germline, reflecting the heterogeneity of induced mutations in P0 founder fish (Fig. 2A,B). By screening for the loss of a restriction site at the target region we might have even missed some mutations that do not affect the restriction enzyme recognition site. To potentially identify mutations induced at off-target sites, we performed next generation sequencing (NGS) of an amplicon of the C9t3 target site from pooled DNA derived from ten C9t3 gRNA/Cas9 mRNA-injected embryos. We found that 50.5% of the mapped reads had an indel mutation at the C9t3 target site (Fig. 2D; supplementary material Fig. S3A). To further determine the mutagenesis frequency at potential off-target sites we analyzed four distinct genomic regions with the highest homology to the target site (off-target sites 1-4). Only 2.2-2.5% of all reads had mutations at the off-target sites in the pool of ten injected embryos (Fig. 2D; supplementary material Fig. S3B). Mutations at off-target sites with closest homology to the target site are infrequent despite the smaller gRNA targeting sequence compared with TALEN and ZFN.

Encouraged by the efficiency and specificity of the CRISPR/Cas9 system we speculated that it might be suitable to facilitate a targeted KI approach in zebrafish. We designed a donor oligonucleotide containing an HA tag flanked by a 41 nt left and a 49 nt right homology arm to introduce the HA tag of the donor oligonucleotide by homologous recombination 3' of the *C13H9orf72* start codon (Fig. 3A). We injected Cas9 mRNA and the gRNA targeting the ATG start codon of *C13H9orf72* (C9t3) together with the HA tag-containing donor oligonucleotide (hereafter referred to as C9t3 KI injected) and screened 20 embryos for successful KI by PCR (supplementary material Fig. S4A). Nine out of 20 injected P0 embryos (45%) were positive by PCR screening for successful KI (Fig. 3B). We next raised the injected embryos and prescreened fin biopsies of adult fish for successful KI (supplementary material Fig. S4A). From four positively prescreened founder fish we recovered two alleles containing the HA tag (supplementary material Fig. S4B). However, both lines had mutations in addition to integration of the HA tag (supplementary material Fig. S4B). None of the 35 negatively prescreened fish had a KI in the F1 generation, validating our approach of prescreening. A systematic analysis of KI parameters was performed by NGS of ten C9t3 KI injected embryos.

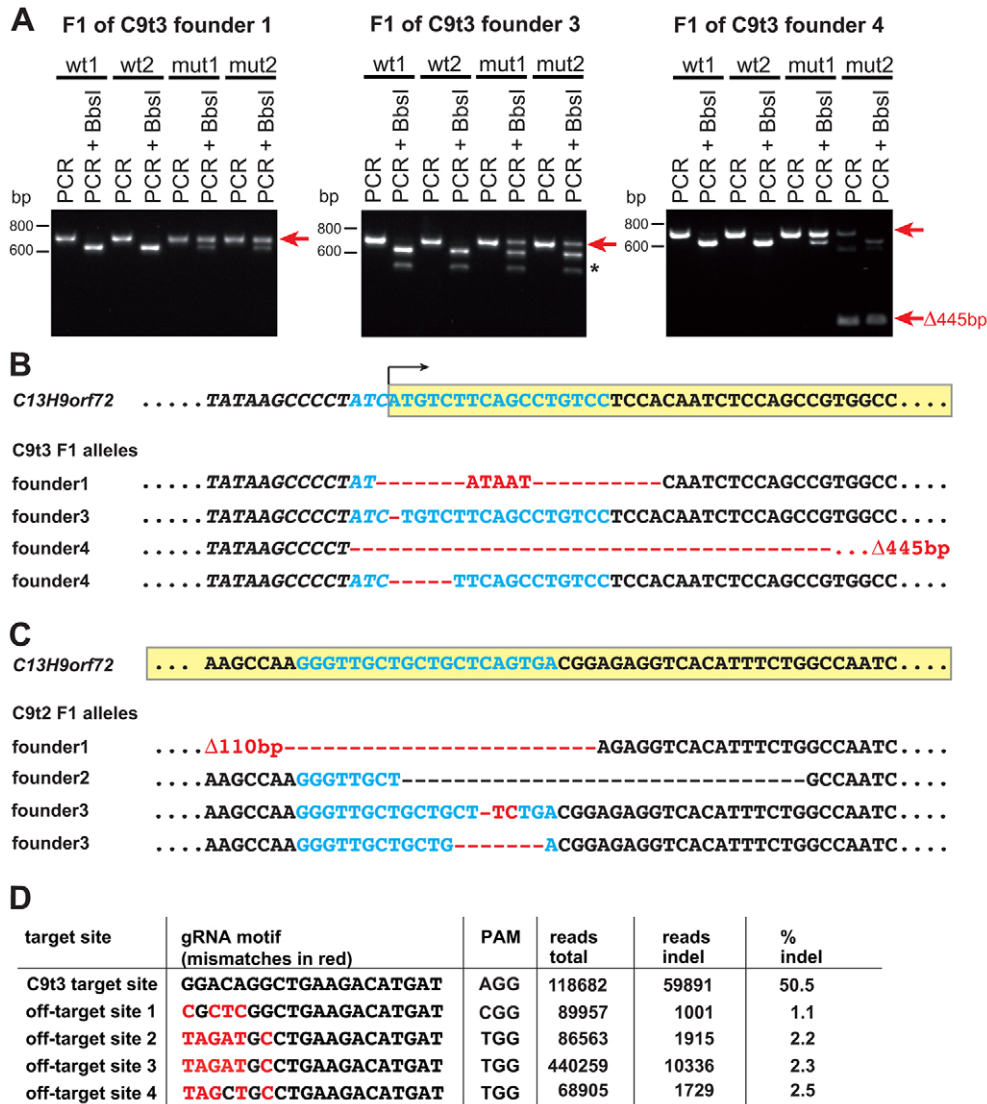


Fig. 2. Germline transmission of CRISPR/Cas9-induced mutations in the *C13H9orf72* locus and on-target and off-target mutagenesis frequencies.

(A) PCR and restriction enzyme analysis of individual F1 embryos obtained from three P0 founder fish (C9t3 P0 founders 1, 3 and 4) that have been injected with C9t3 gRNA/Cas9 mRNA. Lanes 1-4 are wild-type F1 embryos and lanes 5-8 are mutant F1 embryos. Red arrows indicate undigested mutant bands in PCR + BbsI lanes in mutant F1 embryos, which were used for sequencing. Founder 4 gave rise to two different alleles (upper arrow points to the undigested band in lane 6; lower arrow points to the band of the 445 bp deletion in lane 8). Asterisk marks polymorphism. (B,C) Wild-type *C13H9orf72* sequence (top) and sequences derived from the mutant F1 alleles of C9t3 founders 1, 3 and 4 (B) and C9t2 founders 1, 2 and 3 (C). Yellow boxes indicate coding sequence. Target sequence is cyan; mutations are in red. (D) Summary of next generation sequencing (NGS) data derived from the C9t3 gRNA/Cas9 mRNA-injected embryos and the potential off-target sites 1-4. Off-target sites 2 and 3 have a similar genomic environment and identical target sequences.

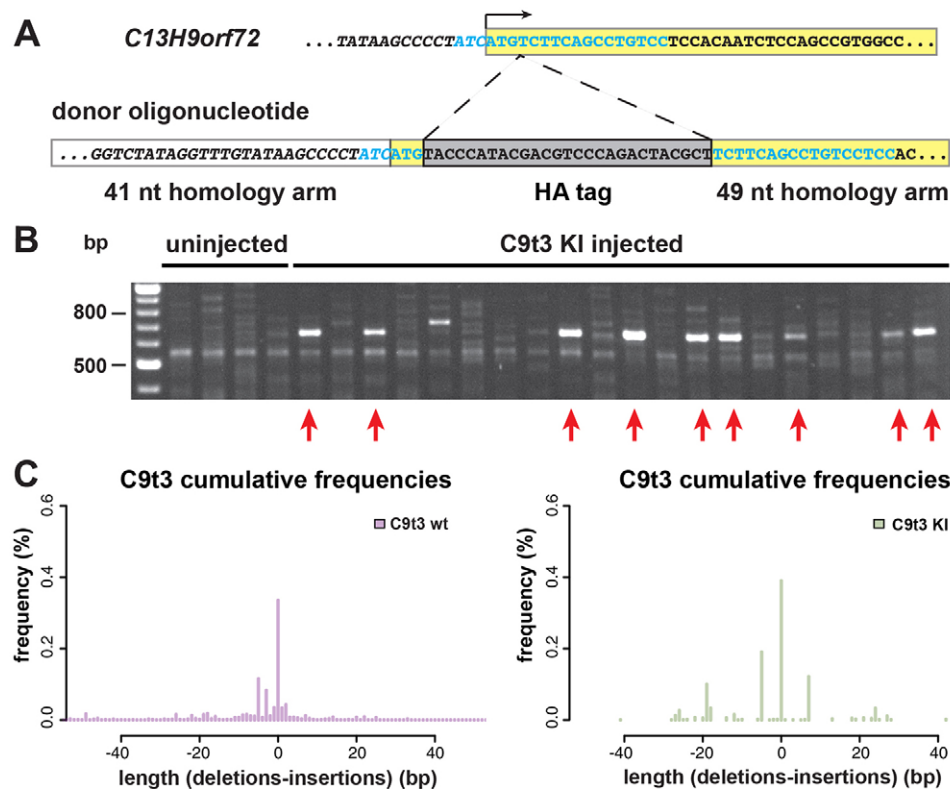
A high rate of mutagenesis (50-76%) of the injected embryos was observed. Additionally, the embryos showed on average a KI rate of 3.5%, of which about half (1.7%) showed correct KI without additional mutations (Fig. 3C,D; supplementary material Fig. S5).

CRISPR/Cas9 is therefore not only efficient to generate mutations in zebrafish but also suitable for KI strategies. However, the inserted HA tag at the C9t3 locus was not detectable by western blot analysis or immunohistochemistry, most likely owing to low expression of the *C13H9orf72* protein. We therefore used a similar strategy at the *bpt1* site, which is actively transcribed and translated (Schmid et al., 2013). We co-injected the *bpt1* gRNA, Cas9 mRNA and a donor oligonucleotide with a 33 nt left homology arm, two HA tags to improve detection sensitivity, and a 33 nt right homology arm (hereafter referred to as *bpt1* KI injected) (Fig. 4A). Fourteen of the 20 (70%) injected embryos analyzed were positive by PCR analysis for the HA tag, indicating successful integration (Fig. 4B).

To determine the KI efficiency at the *bpt1* locus, we subjected ten *bpt1* KI injected embryos to NGS analysis. The efficiency to induce mutations varied between embryos (61-98%) and was on average 86.0% (Fig. 4C; supplementary material Fig. S6). The average HA tag integration rate was 15.6%, but only 3.5% had a correct KI without any additional mutations (Fig. 4F). The high KI efficiency

at the *bpt1* locus is most likely due to the highly efficient *bpt1* gRNA (reaching up to 98% mutagenesis efficiency), increasing the chances of an early double-strand break and donor DNA integration. Consistent with the high mutagenesis rates in the injected founder embryos we detected reduced levels of Tardbp protein by western blot upon *bpt1* KI injection (Fig. 4D). Using a sensitive anti-HA tag antibody we could further detect the Tardbp-HA fusion protein at the expected molecular weight of 44 kDa by western blot in injected founder embryos (Fig. 4D). Importantly, the nuclear localization of Tardbp (Shankaran et al., 2008) was recapitulated by immunohistochemistry with the HA-specific antibody (Fig. 4E).

In conclusion, we have adapted the protocol to efficiently synthesize gRNA without any cloning and show efficient mutagenesis, KI and germline transmission, comparable to TALEN and ZFN approaches (Bedell et al., 2012; Blackburn et al., 2013; Chang et al., 2013; Hwang et al., 2013b). Most importantly, we provide evidence of limited off-target effects and efficient KI, especially upon preselection of founder fish. In contrast to ZFN or TALEN, the design and generation of CRISPR/Cas9 RNAs is much cheaper and less time consuming, making it an excellent genome editing tool, and not only in zebrafish. This system further opens new avenues for the analysis of gene function *in vivo* and for the generation of new disease models in vertebrates.

**Fig. 3. HA tag knock-in at the C9t3 locus.**

(A) The KI strategy at the C9t3 locus. (B) PCR analysis of individual KI injected embryos. Red arrows indicate successful donor oligonucleotide genomic integration.

(C) Average frequencies among ten embryos of C9t3 KI NGS reads mapped to wild-type (wt, left) and KI (right) sequence. In both panels 0 indicates correctly mapped reads without indels (left, 0=wt, no indels; right, 0=correct KI, no indels). Negative values are deletions and positive values are insertions. (D) Summary of NGS data for the C9t3 KI analysis.

D NGS of C9t3 KI injected embryos

reads total	543088
average % reads with mutations	64.1%
average % reads with KI	3.5%
average % reads with correct KI	1.7%

MATERIALS AND METHODS

Zebrafish

Zebrafish (*Danio rerio*) embryos were kept at 28.5°C and were staged according to Kimmel et al. (Kimmel et al., 1995). The wild-type line AB was used. All experiments were performed in accordance with animal protection standards of the Ludwig-Maximilians University Munich and were approved by the government of Upper Bavaria (Regierung von Oberbayern, Munich, Germany).

Guide oligonucleotide

The gRNA antisense oligonucleotide sequence (5'-3') was: *AAAGCACCGACTCGGTGCCACTTTTCAAGTTGATAACGGACTAGCCTTATTTAACTTGCTATTCTAGCTCTAAACNNNNNNNNNNNNNNNNNNNNNNCTATAGTGAGTCGTATTACGC*, with the T7 site shown in bold, N₂₀ indicating the targeting sequence, and the gRNA scaffold adopted from Mali et al. (Mali et al., 2013) shown in italics (see Fig. 1A; supplementary material Fig. S1A).

The targeting sequences (N₂₀) used for the respective gRNA (in parenthesis) were: *tardbp* targeting oligo 1 (bpt1), CCCATGTGCTT-CGGCTGCC; *tardbp1* targeting oligo 4 (bpt4), AACTACTCTGAAGTGC-TGCC; *C13H9orf72* targeting oligo 2 (C9t2), TCACTGAGCAGCAGCA-ACCC; and *C13H9orf72* targeting oligo 3 (C9t3), ATCATGTCTTCA-GCCTGTCC.

For direct *in vitro* transcription, the gRNA antisense oligonucleotide was annealed to the T7 primer (TAATACGACTCACTATAG; 5 minutes at 95°C, then cooled at room temperature for 5 hours) and *in vitro* transcribed using the Ambion MEGAscript-T7 kit.

The gRNA antisense oligonucleotide was PCR amplified for cloning with primer 1 (CGTAATACGACTCACTATAG) and primer 2 (which adds a *DraI* restriction site, CGCGTTAAAGCACCGACTCGGTGCCAC) and

the PCR product gel-purified and subcloned into pCR8/GW/TOPO/TA (Invitrogen). The insert was excised using *DraI* and *ApaI* (NEB). The excised insert and PCR product were *in vitro* transcribed using the MEGAscript-T7 kit.

Cas9

Nuclear localization sequences on both ends and one C-terminal HA tag were added to wild-type Cas9 from *Streptococcus pyogenes* (Addgene, 39312) by PCR (supplementary material Fig. S1C) using primer 1 (ATGGCCCCAAAGAAGAAGCGCAAGGTAGGTGGAGGTGGAGGAG-GAGATAAGAAATACTCAATAGGCTTAG) and primer 2 (TCAAGCGT-AGTCTGGGACGTCGTATGGGTAACCTCCTCCTCCTCCTACCTT-ACGCTTCTTCTTGGAGCACCTCCTCCTCCTCCTCCGTCACCTCCT-AGTGACT). The PCR product was subcloned into a pCR8/GW/TOPO/TA vector (Invitrogen) and further recombined into pCS2+/GW using LR Clonase II (Invitrogen). After linearization with *ApaI* (NEB), Cas9 was *in vitro* transcribed using the SP6 mMESSAGE mMACHINE kit (Ambion).

Microinjection and knock in

gRNAs were microinjected (Femtojet, Eppendorf) at a final concentration of 2.4 µg/µl together with 0.5 µg/µl Cas9 mRNA into fertilized one-cell stage embryos. For KI, 100 nM donor oligonucleotide was co-injected. Uninjected siblings were used as controls. Oligonucleotides were (HA tag sequence in bold): donor oligonucleotide for C9t3 (120 nt), CTTC-TGCTTTGTGAGCCTGACGGTCTATAGGTTGTATAAGCCCCATC-ATGTACCACATACGACGTCCAGACTACGCTTCTCAGCCTGTC-ATCCACAATCTCCAGCCGTGGCCAAGAC; and donor oligonucleotide for bpt1 (120 nt), GGTCAGGGTTTTGCAGGCAGCCGAAGCAACATG-TACCACATACGACGTCCAGACTACGCTTACCACATACGACGTCC-CAGACTACGCTGGTGGTGGTGGGGGTAGCTCCAGCAGTTG.

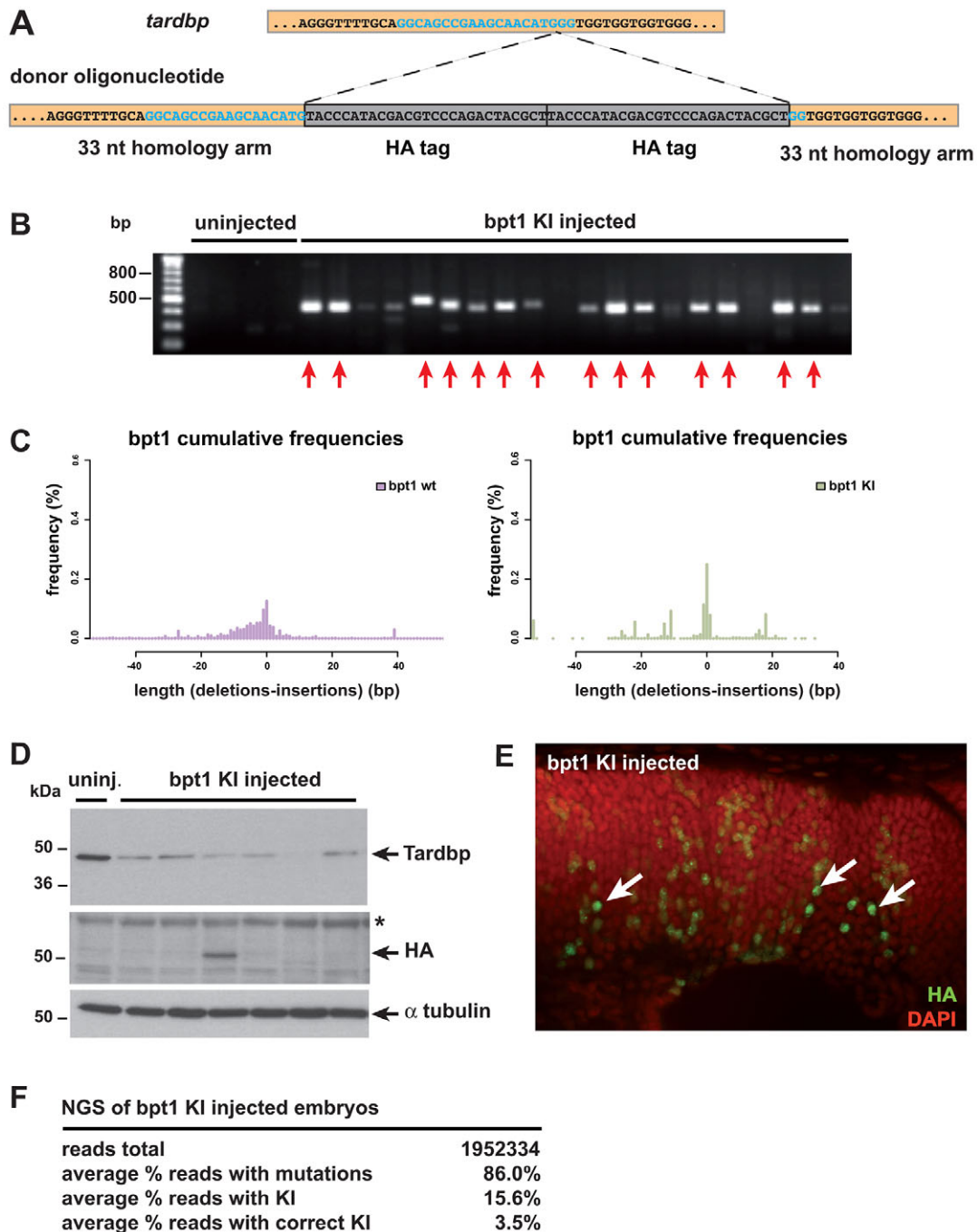


Fig. 4. HA tag knock-in at the *bpt1* locus. (A) The KI strategy at the *bpt1* locus. (B) PCR analysis of KI injected embryos. Red arrows indicate successful genomic integration of the HA tag derived from the donor oligonucleotide. (C) Average frequencies of NGS reads of ten *bpt1* KI embryos mapped to wild-type (left) and KI reference (right) sequence. Negative values are deletions and positive values are insertions. (D) Western blot analysis of *bpt1* KI embryos with antibodies against Tardbp, HA and α -tubulin. Asterisk indicates unspecific bands. (E) Immunohistochemistry of 2 dpf *bpt1* KI injected embryos with antibodies against the HA epitope (green) counterstained with DAPI (red). Arrows indicate HA-positive nuclear staining. (F) Summary of NGS data for the *bpt1* KI analysis.

PCR analysis

DNA of 1 dpf embryos was used as a template for PCR with the following primers: C13H9orf72-for (genotyping C9t2 and C9t3), GCAATCTGTT-TGTCCCACT; C13H9orf72-rev (genotyping C9t2 and C9t3), ATCA-ACCTCCTCTGGCACAC; *tardbp*-for (genotyping *bpt1*), GAAGAAAT-TTCCAACCTTCTTTC; *tardbp*-rev (genotyping *bpt1*), ACTTACCAAAAC-ACGCTAGG; *tardbp1*-for (genotyping *bpt4*), GCCTAAGCACAAATAAT-AGTAGG; *tardbp1*-rev (genotyping *bpt4*), CTCTACTACCACTCTGC; C9t3-HA-tag-for (genotyping HA KI C9t3), CCCTATCATGTACCCA-TACG; 2x-HA-tag-for (genotyping HA KI *bpt1*), CTTACCCATACGAC-

GTCC; and *tardbp*-rev (genotyping HA KI in *bpt1*), ACTTACCAAAAC-ACGCTAGG.

For RFLP analysis, half of the PCR product was digested with the following enzymes (NEB): *tardbp* (*bpt1*), *CspCI*; *tardbp1* (*bpt4*), *Hpy188I*; *C13H9orf72* (C9t2), *DdeI*; *C13H9orf72* (C9t3), *BbsI*.

Next generation sequencing

Putative off-target sites of the C9t3 gRNA were identified by BLAST search of the 13 nt 5' of the PAM motif containing an NGG motif (previously described to be crucial for binding) (Cong et al., 2013; Jinek et al., 2012)

using Ensembl Genome assembly Zv9 (GCA_000002035.2). The DNA of ten individual embryos injected with Cas9 and C9t3 gRNA was pooled and analyzed for C9t3 gRNA target effects and off-target effects. From this pool we PCR amplified the C9t3 locus and the four potential off-target sites (supplementary material Fig. S3). Ten individual embryos injected with C9t3 gRNA, Cas9 mRNA and the donor oligonucleotide were PCR amplified and analyzed individually for KI efficiency (supplementary material Fig. S5). Adapter ligation, sequencing and tag sorting were performed by GATC Biotech (Germany). KI analysis at the *bpt1* locus was performed (supplementary material Fig. S6). The length of the expected PCR products varied between 184 bp and 417 bp. We sequenced on a MiSeq platform (Illumina) in paired-end mode of appropriate length (140 bp or 250 bp). Templates of the C9t3 gRNA target sites and potential off-target sites were used as a reference sequence for determination of the off-target lesions (supplementary material Fig. S3). Templates of *bpt1* and C9t3 with and without inserted HA tags and the C9t3-associated off-target sites were used as reference sequences for determination of KI efficiency (supplementary material Figs S5, S6). Reference-guided sequence assemblies were performed with Novoalign (v3, Novocraft). The frequency of insertions and deletions around the best-matching reference sequence was derived from the CIGAR code of the sequence alignments (Java and R scripts for statistical evaluation are available upon request). Primers used for barcode labeling are also available upon request.

Western blot analysis and immunohistochemistry

Western blotting (WB) and immunohistochemistry (IHC) were performed as previously described (Schmid et al., 2013). Primary antibodies used: Tardbp 4A12-111 (Tardbp epitope: TSTSGTSSSRDQAQTY), WB 1:1; α -tubulin (Sigma, T6199), WB 1:8000; HA.11 (Covance, MMS-101P), WB 1:2000, IHC 1:200.

Acknowledgements

We thank D. Edbauer, P.-H. Kuhn, R. Kühn, B. Solchenberger, S. Rothhämel and F. van Bebber for critically reading the manuscript and R. Rojas Rojas for zebrafish care.

Competing interests

The authors declare no competing financial interests.

Author contributions

A.H., C.H. and B.S. designed experiments. A.H., A.R., P.K., V.H. and J.H. performed experiments. A.H., P.K., C.H. and B.S. wrote the paper.

Funding

The research leading to these results has received funding from the European Research Council under the European Union Seventh Framework Programme [FP7/2007-2013]/ERC grant agreement no 321366-Amyloid to C.H. and the Center of Excellence in Neurodegeneration (COEN) to C.H. and B.S.

Supplementary material

Supplementary material available online at <http://dev.biologists.org/lookup/suppl/doi:10.1242/dev.099085/-/DC1>

References

- Bedell, V. M., Wang, Y., Campbell, J. M., Poshusta, T. L., Starker, C. G., Krug, R. G., 2nd, Tan, W., Penheiter, S. G., Ma, A. C., Leung, A. Y. et al. (2012). In vivo genome editing using a high-efficiency TALEN system. *Nature* **491**, 114-118.
- Blackburn, P. R., Campbell, J. M., Clark, K. J. and Ekker, S. C. (2013). The CRISPR system – keeping zebrafish gene targeting fresh. *Zebrafish* **10**, 116-118.
- Carroll, D. (2011). Genome engineering with zinc-finger nucleases. *Genetics* **188**, 773-782.
- Chang, N., Sun, C., Gao, L., Zhu, D., Xu, X., Zhu, X., Xiong, J. W. and Xi, J. J. (2013). Genome editing with RNA-guided Cas9 nuclease in zebrafish embryos. *Cell Res.* **23**, 465-472.
- Cho, S. W., Kim, S., Kim, J. M. and Kim, J. S. (2013). Targeted genome engineering in human cells with the Cas9 RNA-guided endonuclease. *Nat. Biotechnol.* **31**, 230-232.
- Cong, L., Ran, F. A., Cox, D., Lin, S., Barretto, R., Habib, N., Hsu, P. D., Wu, X., Jiang, W., Marraffini, L. A. et al. (2013). Multiplex genome engineering using CRISPR/Cas systems. *Science* **339**, 819-823.
- DeJesus-Hernandez, M., Mackenzie, I. R., Boeve, B. F., Boxer, A. L., Baker, M., Rutherford, N. J., Nicholson, A. M., Finch, N. A., Flynn, H., Adamson, J. et al. (2011). Expanded GGGGCC hexanucleotide repeat in noncoding region of C9ORF72 causes chromosome 9p-linked FTD and ALS. *Neuron* **72**, 245-256.
- Gaj, T., Gersbach, C. A. and Barbas, C. F., III (2013). ZFN, TALEN, and CRISPR/Cas-based methods for genome engineering. *Trends Biotechnol.* **31**, 397-405.
- Gijselink, I., Van Langenhove, T., van der Zee, J., Slegers, K., Philtjens, S., Kleinberger, G., Janssens, J., Bettens, K., Van Cauwenbergh, C., Pereson, S. et al. (2012). A C9orf72 promoter repeat expansion in a Flanders-Belgian cohort with disorders of the frontotemporal lobar degeneration-amyotrophic lateral sclerosis spectrum: a gene identification study. *Lancet Neurol.* **11**, 54-65.
- Horvath, P. and Barrangou, R. (2013). RNA-guided genome editing à la carte. *Cell Res.* **23**, 733-734.
- Hwang, W. Y., Fu, Y., Reyon, D., Maeder, M. L., Kaini, P., Sander, J. D., Joung, J. K., Peterson, R. T. and Yeh, J. R. (2013a). Heritable and precise zebrafish genome editing using a CRISPR-Cas system. *PLoS ONE* **8**, e68708.
- Hwang, W. Y., Fu, Y., Reyon, D., Maeder, M. L., Tsai, S. Q., Sander, J. D., Peterson, R. T., Yeh, J. R. and Joung, J. K. (2013b). Efficient genome editing in zebrafish using a CRISPR-Cas system. *Nat. Biotechnol.* **31**, 227-229.
- Jao, L. E., Wente, S. R. and Chen, W. (2013). Efficient multiplex biallelic zebrafish genome editing using a CRISPR nuclease system. *Proc. Natl. Acad. Sci. USA* (in press), doi: 10.1073/pnas.1308335110.
- Jinek, M., Chylinski, K., Fonfara, I., Hauer, M., Doudna, J. A. and Charpentier, E. (2012). A programmable dual-RNA-guided DNA endonuclease in adaptive bacterial immunity. *Science* **337**, 816-821.
- Jinek, M., East, A., Cheng, A., Lin, S., Ma, E. and Doudna, J. (2013). RNA-programmed genome editing in human cells. *eLife* **2**, e00471.
- Joung, J. K. and Sander, J. D. (2013). TALENs: a widely applicable technology for targeted genome editing. *Nat. Rev. Mol. Cell Biol.* **14**, 49-55.
- Kimmel, C. B., Ballard, W. W., Kimmel, S. R., Ullmann, B. and Schilling, T. F. (1995). Stages of embryonic development of the zebrafish. *Dev. Dyn.* **203**, 253-310.
- Mali, P., Yang, L., Esvelt, K. M., Aach, J., Guell, M., DiCarlo, J. E., Norville, J. E. and Church, G. M. (2013). RNA-guided human genome engineering via Cas9. *Science* **339**, 823-826.
- Mori, K., Weng, S. M., Arzberger, T., May, S., Rentzsch, K., Kremmer, E., Schmid, B., Kretzschmar, H. A., Cruts, M., Van Broeckhoven, C. et al. (2013). The C9orf72 GGGGCC repeat is translated into aggregating dipeptide-repeat proteins in FTLD/ALS. *Science* **339**, 1335-1338.
- Renton, A. E., Majounie, E., Waite, A., Simón-Sánchez, J., Rollinson, S., Gibbs, J. R., Schymick, J. C., Laaksvirta, H., van Swieten, J. C., Myllykangas, L. et al.; ITALSGEN Consortium (2011). A hexanucleotide repeat expansion in C9ORF72 is the cause of chromosome 9p21-linked ALS-FTD. *Neuron* **72**, 257-268.
- Schmid, B., Hruscha, A., Hög, S., Banzhaf-Strathmann, J., Strecker, K., van der Zee, J., Teucke, M., Eimer, S., Hegermann, J., Kittelmann, M. et al. (2013). Loss of ALS-associated TDP-43 in zebrafish causes muscle degeneration, vascular dysfunction, and reduced motor neuron axon outgrowth. *Proc. Natl. Acad. Sci. USA* **110**, 4986-4991.
- Shankaran, S. S., Capell, A., Hruscha, A. T., Fellerer, K., Neumann, M., Schmid, B. and Haass, C. (2008). Missense mutations in the progranulin gene linked to frontotemporal lobar degeneration with ubiquitin-immunoreactive inclusions reduce progranulin production and secretion. *J. Biol. Chem.* **283**, 1744-1753.
- Shen, B., Zhang, J., Wu, H., Wang, J., Ma, K., Li, Z., Zhang, X., Zhang, P. and Huang, X. (2013). Generation of gene-modified mice via Cas9/RNA-mediated gene targeting. *Cell Res.* **23**, 720-723.
- van Bebber, F., Hruscha, A., Willem, M., Schmid, B. and Haass, C. (2013). Loss of Bace2 in zebrafish affects melanocyte migration and is distinct from Bace1 knock out phenotypes. *J. Neurochem.* (in press). doi: 10.1111/jnc.12198.
- Wang, H., Yang, H., Shivalila, C. S., Dawlaty, M. M., Cheng, A. W., Zhang, F. and Jaenisch, R. (2013). One-step generation of mice carrying mutations in multiple genes by CRISPR/Cas-mediated genome engineering. *Cell* **153**, 910-918.
- Wiedenheft, B., Sternberg, S. H. and Doudna, J. A. (2012). RNA-guided genetic silencing systems in bacteria and archaea. *Nature* **482**, 331-338.